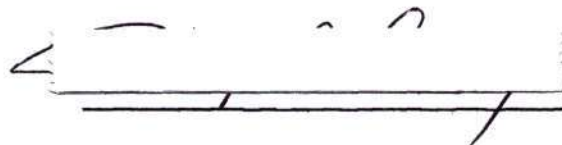


In presenting the dissertation as a partial fulfillment of the requirements for an advanced degree from the Georgia Institute of Technology, I agree that the Library of the Institute shall make it available for inspection and circulation in accordance with its regulations governing materials of this type. I agree that permission to copy from, or to publish from, this dissertation may be granted by the professor under whose direction it was written, or, in his absence, by the Dean of the Graduate Division when such copying or publication is solely for scholarly purposes and does not involve potential financial gain. It is understood that any copying from, or publication of, this dissertation which involves potential financial gain will not be allowed without written permission.



7/25/68

DEVELOPMENT OF COMPRESSIVE SURFACE STRESSES  
IN SLIP-CAST FUSED SILICA

A THESIS

Presented to

The Faculty of the Graduate Division

by

Phillip A. Ormsby

In Partial Fulfillment

of the Requirements for the Degree

Master of Science in Ceramic Engineering

Georgia Institute of Technology

June, 1969

DEVELOPMENT OF COMPRESSIVE SURFACE STRESSES

IN SLIP-CAST FUSED SILICA

Approv

Chairman

Date Approved by Chairman May 16, 1969

## ACKNOWLEDGMENTS

I should like to take this opportunity to thank Dr. Willis E. Moody for his time and constructive criticism throughout my graduate program.

I also thank Dr. Lane Mitchell and Dr. Allen T. Chapman for their participation on my reading committee.

I wish to express my appreciation to the staff at the High Temperature Materials Division, Engineering Experiment Station, for the use of their facilities and their freely offered assistance in the experimental phase of this effort.

I should also like to thank Dr. William J. Corbett of Thermo Materials Corporation for his suggestion and the fused silica slips used in these experiments.

I should especially like to express my appreciation to my wife whose understanding and encouragement have made this effort possible.

## TABLE OF CONTENTS

	Page
ACKNOWLEDGMENTS .....	ii
LIST OF TABLES .....	iv
LIST OF ILLUSTRATIONS .....	v
SUMMARY .....	vi
Chapter	
I. INTRODUCTION .....	1
II. REVIEW OF LITERATURE .....	3
Development of Strengthening Concepts	
Characteristics of Silica	
Application of Concepts to Slip-Cast Fused Silica	
III. INSTRUMENTATION AND EQUIPMENT .....	14
Norelco X-ray Diffraction Facility	
Numico Air Porosimeter	
Baldwin and Instron Universal Test Machine	
Resonant Frequency Measurement Facility	
IV. PROCEDURE .....	15
Introduction	
Approach	
Experimental Techniques	
Specimen Preparation	
Evaluation of Specimens	
V. DISCUSSION OF RESULTS .....	38
VI. CONCLUSIONS .....	46
BIBLIOGRAPHY .....	48

## LIST OF TABLES

Table		Page
1.	Characterization Data on Selected Fused Silica Slips, and Test Specimens Produced Using Them . . . . .	18
2.	Slip-Characterization Data Obtained from 2300° F Sintering Temperature . . . . .	19
3.	Modulus of Rupture Results from Studies on Thickness of Skin for Composites . . . . .	22
4.	Sintering Schedules, Batch Numbers, and Compositions . . . . .	24
5.	Modulus of Rupture Data Depicting Decreased Standard Deviation Exhibited by Composites . . . . .	28
6.	Physical Properties for Specimens Fired in Furnace With Rotating Hearth . . . . .	28
7.	Data on Specimens Sintered at 2200° F . . . . .	29
8.	Physical Properties of Specimens Sintered at 2300° F . . . . .	29
9.	Modulus of Rupture Data for Quenched Specimens . . . . .	30
10.	Deflections Measured in Slotted Bar Stress Relief Test . . . . .	31
11.	ASTM Powder Index Data for Cristobalite . . . . .	35

## LIST OF ILLUSTRATIONS

Figure		Page
1.	Stability Relationships for Different Phases of Silica . . . . .	6
2.	Viscosity-Temperature Curves. . . . .	8
3.	Specific Volumes of Cristobalite and Fused Silica Compared . . . . .	10
4.	Elevated Temperature Impact Strength of Silica . . . . .	12
5.	Elevated Temperature Tensile Strengths of Various Forms of Silica . . . . .	13
6.	Illustration of Split Rod Test . . . . .	36
7.	Composite Specimen, Slip 2 Over 1 . . . . .	41
8.	Composite Specimen, Slip 1 Over 2 . . . . .	41
9.	Modulus of Rupture Versus Time at Sintering Temperature . . . . .	44



## SUMMARY

Compressive surface stresses have been used for many years to strengthen glassy ceramics. An attempt was made to develop compressive surface stresses in slip-cast fused silica to increase its load-carrying capabilities.

The method used to accomplish this was based on the development of stresses in a silica composite by causing the center portion of a cylindrical specimen to contract more than the exterior shell. This was accomplished by preparing specimens with two fused silica slips having different particle sizes, or different devitrification rates. The different particle sizes provided a differential sintering shrinkage, while variations in devitrification rates led to different cristobalite contents and resulted in a differential contraction as the specimens were cooled through the cristobalite inversion temperature.

Modulus of rupture tests were used to evaluate these specimens and values obtained for several groups of composites had increased mean strengths and/or decreased standard deviations. Although the strength increases were not as high as predicted, the standard deviations were significantly lower (40-80) for the composites compared with single phase specimens (600-1200). Strength variability is often related to surface flaws, and the reduction in variability suggests that the effect of surface flaws on the composite specimens has been significantly reduced, as a result of the development of compressive prestress.



## CHAPTER I

### INTRODUCTION

During the last three decades, advances in general materials technology have in a large part been paced by the demands of the aerospace industry. Many of the new material advances have been utilized by consumer industries, but the driving force for the rapid generation of new and improved materials has been the ever increasing demands exerted by the aerospace industry. The extreme thermal environments caused by aerodynamic heating of surface structures or by the exhaust products of rocket engines have led to the development of many special super alloys and ablative type organic composites. Ceramics, the most obvious class of materials for high temperature applications, have also been extensively investigated. However, actual use of ceramics for aerospace hardware has usually been limited to very specific applications after all other (non-ceramic) materials were unsuccessful in satisfying the operational requirements. The reluctance of the design engineer to utilize ceramics can usually be related to the generally accepted but not necessarily true belief in the weaknesses of these materials. Ceramics often exhibit poor structural characteristics in any stress state except compression. In many cases when the mean strength appears satisfactory, the individual strength values measured for a given batch of test specimens will often exhibit scatter so extensive that the designer has very limited design

numbers. These limitations often result in the necessity for 100 per cent testing of components to provide the reliability required for most aerospace hardware. Although the scatter and even the relatively low strength values may be attributed in part to the test methods (1), it is apparent that these limitations have resulted in only limited use of ceramics by the aerospace industry. It is also obvious that the role of ceramics in future missiles and rockets must be expanded if the operational goals of these systems are to be achieved. With the strength characteristics limiting the current use of ceramics, it is apparent that these characteristics must be improved in order to utilize the full potential of ceramics for these applications.

The purpose of this effort has been to investigate techniques for improving the strength characteristics of ceramics. Of current interest within the aerospace community, slip-cast fused silica exhibits potential for many future missile applications. Realization of these potentials will require increases in strength and/or improvements in strength reproducibility. Therefore, slip-cast fused silica was selected as an appropriate material for study. Experimental techniques capable of producing a compressive prestress condition in the surface of cylindrical test specimens were investigated. It was postulated that the development of this type of prestress condition in the surface of a ceramic should reduce the effect of flaws and surface discontinuities on the strength characteristics. Specifically, the mean strength should be increased and the scatter in individual strength values should be significantly reduced.

## CHAPTER II

### REVIEW OF LITERATURE

#### Development of Strengthening Concepts

An understanding of the known factors which have influence on mechanical properties of ceramics was essential to the development of an experimental plan for the improvement of these properties. An excellent review of the intrinsic characteristics of ceramics with relation to various properties was presented in the Materials Advisory Board publication "Ceramic Processing" (2). A recent article by Hall (3) also described these relationships and provided additional background on strengthening mechanisms. The predominance of surface related factors in these discussions indicated the impact which general surface state has on strength characteristics. The effect of surface discontinuities (flaws) on the strength of a ceramic is not a new realization, for only simple mechanical relationships are required to illustrate development of significant stress concentrations around these flawed areas. It is notable that although the existence of this source of weakness for ceramics was recognized many years ago, the potential magnitude of the weakness has only recently been observed. Fletcher and Tillman (4), for example, observed order of magnitude strength increases in soda-lime glass rods by simple acid etching (16,000 to 300,000 psi). Other treatments, including quenching in silicone and



hydrocarbon oils, also produced strength increases which were not as significant. These experiments indicated that the strength for soda-lime glass rods could be greatly increased by smoothing out the discontinuities by etching or, to lesser degree, by the formation of stresses during quenching. The quenching phenomena caused the development of stresses through differential cooling and solidification of the surface and the core of glass. This phenomenon is also discussed by Weyman (5) and Barsom (6) in their articles on tempered glasses.

Duke (7) described the application of glazes on compositions having different thermal expansion characteristics. This technique produced compressive stresses in the glaze and thereby increased the external tensile load required to cause nucleation of cracks.

Kirchner's research (8, 9, 10) on chemical strengthening also supports the basic postulate relating strength to surface condition. A variety of experimental procedures was investigated in attempting to strengthen alumina, spinels, titania, silica, and glassy silicates. Each experiment was based on the formation of compressive surface layers to increase strength. Typical techniques used by Kirchner included diffusion impregnation, glazing, quenching, and surface etching. Indications of apparent strength increases of 10 per cent were presented.

Kistler (11) and Nordberg (12) describe the strengthening of glasses by ion exchange. In these experiments, compressive surface stresses were

obtained by exchange of the sodium monovalent ions by larger sized ions (potassium, cesium) of the same charge. This "stuffing" technique, diffusion into surface from solutions below strain temperature, caused compressive stresses to be developed as the larger ion attempted to fit into the hole sized for the sodium ion in the glass network. Strength increases of 300 to 500 per cent were shown by Nordberg since the failure of these surfaces did not occur until the compressive prestress had been overcome.

#### Characteristics of Silica

Sosman (13) and Wilson (14) discuss the polymorphism of silica minerals and present characteristics for the various forms or phases currently cataloged. A typical presentation of the stability of the principal forms of silica as a function of temperature is shown in Figure 1. The phases described in this figure and their relative stability at any specific temperature requires consideration of the rate of change from one phase to another. Changes from  $\alpha$  to  $\beta$  (high-low) forms are relatively rapid and positive upon reaching the critical temperature, while inversions involving more significant change in character (i. e., quartz to cristobalite, silica glass to cristobalite, etc.) are quite sluggish, often requiring hours or days at temperatures outside the stability range of the original phase. Other characteristics of silica important to this investigation include the variations in specific gravity (also presented in Figure 1) for the various phases of silica, and the effect of temperature on the viscosity of silica. Typical viscosity data published by Corning Glass





Works (15) for glass materials are presented in Figure 2. Four points on the viscosity temperature curve were arbitrarily chosen to represent important points in its change from solid to liquid. Definitions used by this manufacturer, as tentatively adopted by the American Society for Testing Materials, are:

#### Strain Point

The temperature, at the lower end of the annealing range, at which the internal stress is substantially relieved in 4 hours. The strain point corresponds to a viscosity of  $10^{14.50}$  poises when measured by the Tentative Method of Test for Annealing Point and Strain Point of Glass (A.S.T.M. Designation: C. 336).

#### Annealing Point

The temperature, at the upper end of the annealing range, at which the internal stress is substantially relieved in 15 minutes. The annealing point corresponds to a viscosity of  $10^{13.00}$  poises when measured by the Tentative Method of Test for Annealing Point and Strain Point of Glass (A.S.T.M. Designation: C. 336).

#### Softening Point

The temperature at which a uniform fiber, 0.55 to 0.74 millimeter in diameter and 23.5 centimeters in length, elongates under its own weight at a rate of 1 millimeter per minute when the upper 10 centimeters of its length is heated in the manner prescribed in the Tentative Method of Test for Softening Point of Glass (A.S.T.M. Designation: C. 338) at a rate of approximately  $5^{\circ}\text{C}$

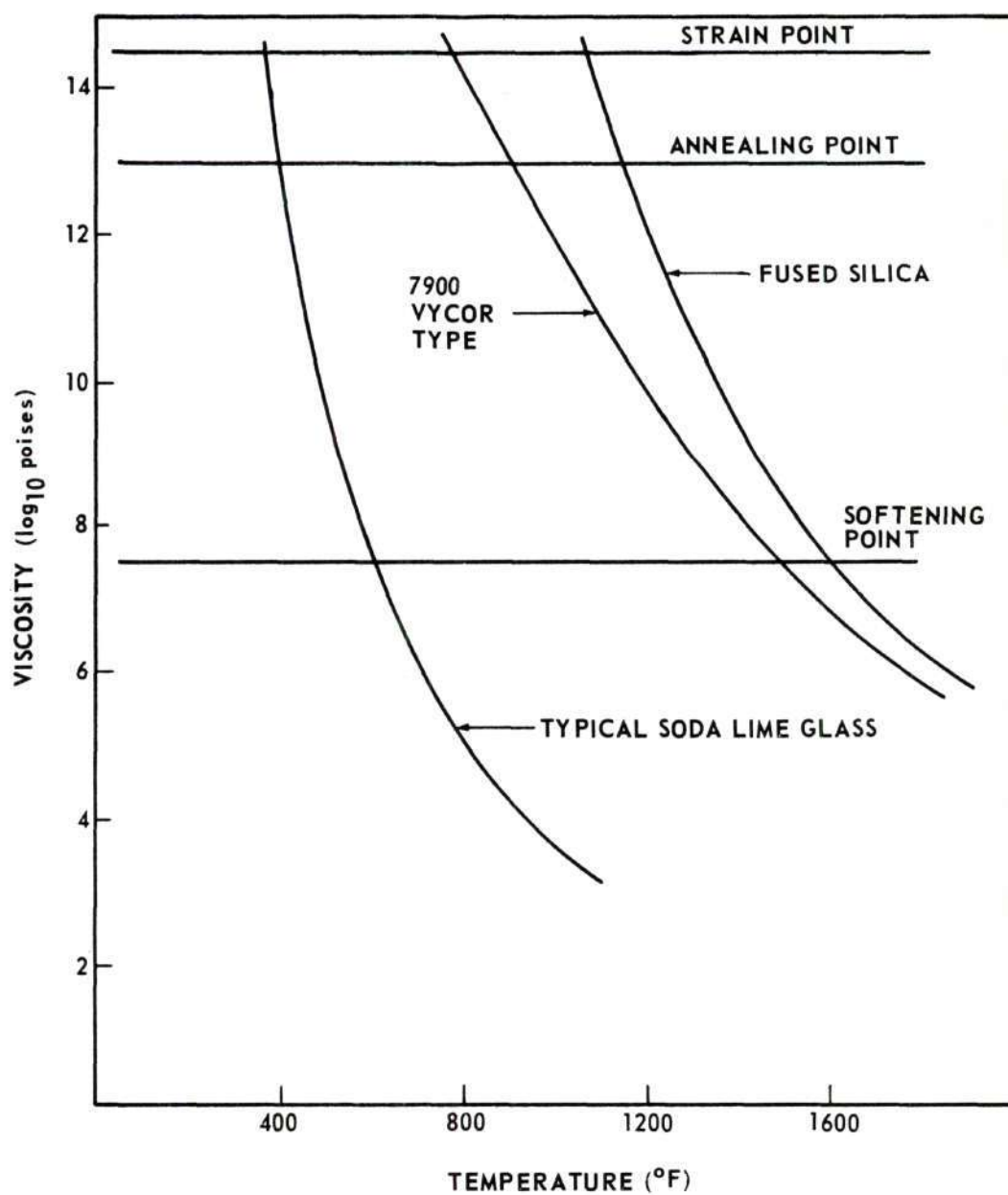


Figure 2. Viscosity-Temperature Curves

per minute. For glass of density near  $2.5 \text{ gm./cm.}^3$  this temperature corresponds to a viscosity of  $10^{7.6}$  poises.

### Working Point

The temperature at which the glass is soft enough for hot working by most of the common methods. Viscosity at the working point is  $10^4$  poises.

### Application of Concepts to Slip-Cast Fused Silica

Sosman's (16) extensive dissertations on the phase transformations of silica indicated the possibility of using these phenomena to provide a shrinkage differential in a multiphase silica body. The particular transformation of interest is the inversion from  $\beta$  to  $\alpha$  cristobalite which occurs at approximately  $270^\circ\text{C}$ . Day, Sosman, and Hostetter (17) showed that this inversion has an accompanying reduction in specific volume of approximately 5 per cent, as illustrated in Figure 3.

Wagstaff (18), Murphy (19), Fleming (20), Brown (21), and Boland (22) have discussed the causes and effects of devitrification of fused silica, and all agree that impurities play a major role in the devitrification rate. Murphy revealed that castings prepared from different slips processed showed significantly different rates of devitrification.

Uhlman (23) discussed the unusual increase in elastic modulus, with increasing temperature (to  $1000^\circ\text{C}$ ) for fused silica and compared it with the normal loss in strength exhibited by most glasses in the same thermal environments. Uhlman also presented data which indicated a strong dependence of all

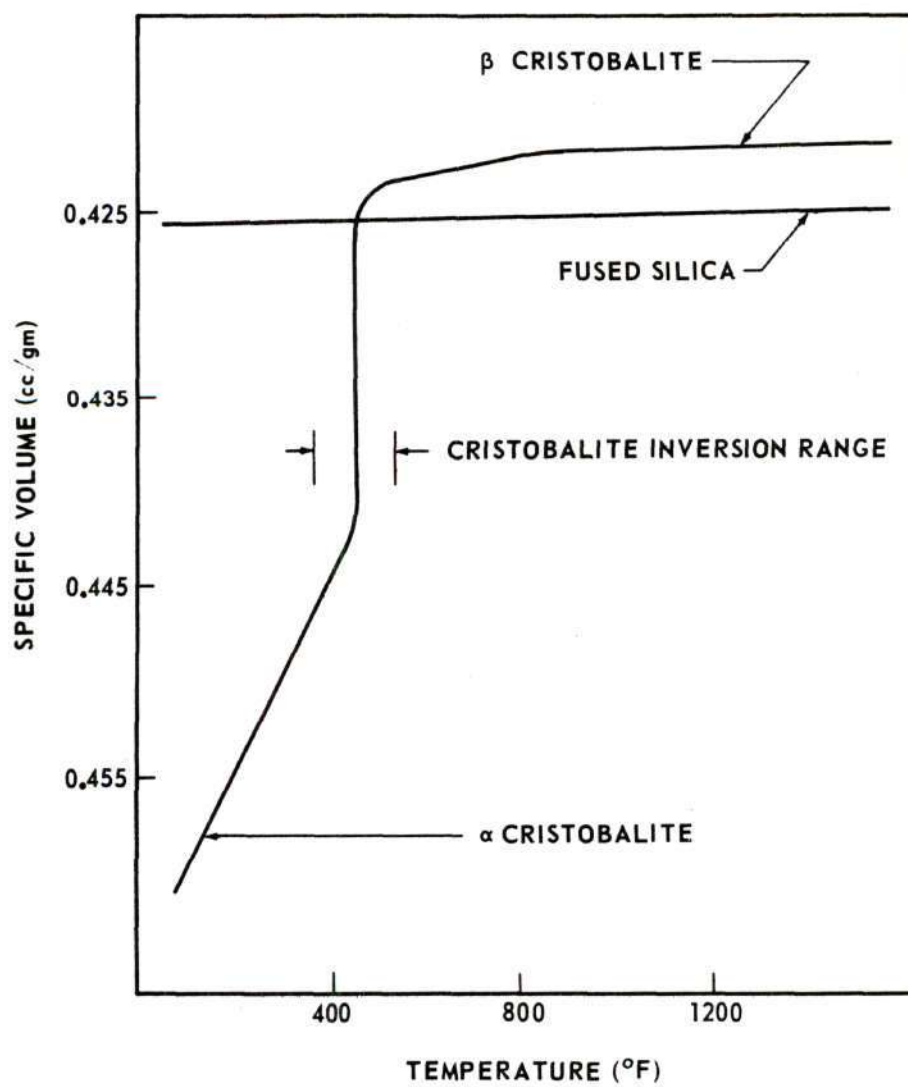


Figure 3. Specific Volumes of Cristobalite and Fused Silica Compared

properties of fused silica on its past thermal history. For example, the viscosity temperature relationship was said to vary as much as two orders of magnitude as a function of the equilibrium temperature (temperature of fusion formation).

Fleming (24) reviewed additional physical property data showing characteristic increases in tensile and impact strengths with increasing temperatures. He also presented data showing the variations in these properties and their temperature dependence for clear fused silica and slip-cast fused silica. This information is presented in Figures 4 and 5.

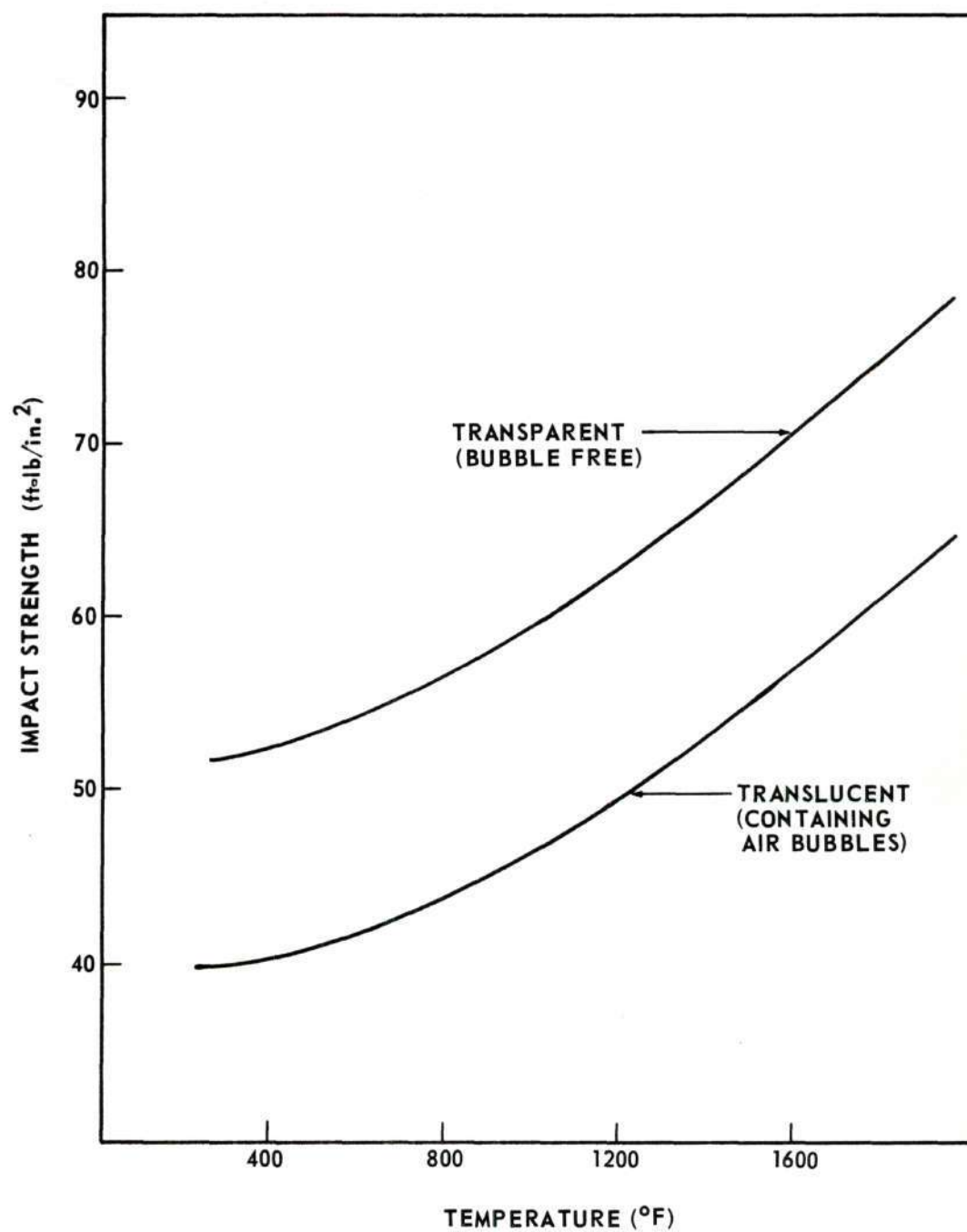


Figure 4. Elevated Temperature Impact Strength of Silica



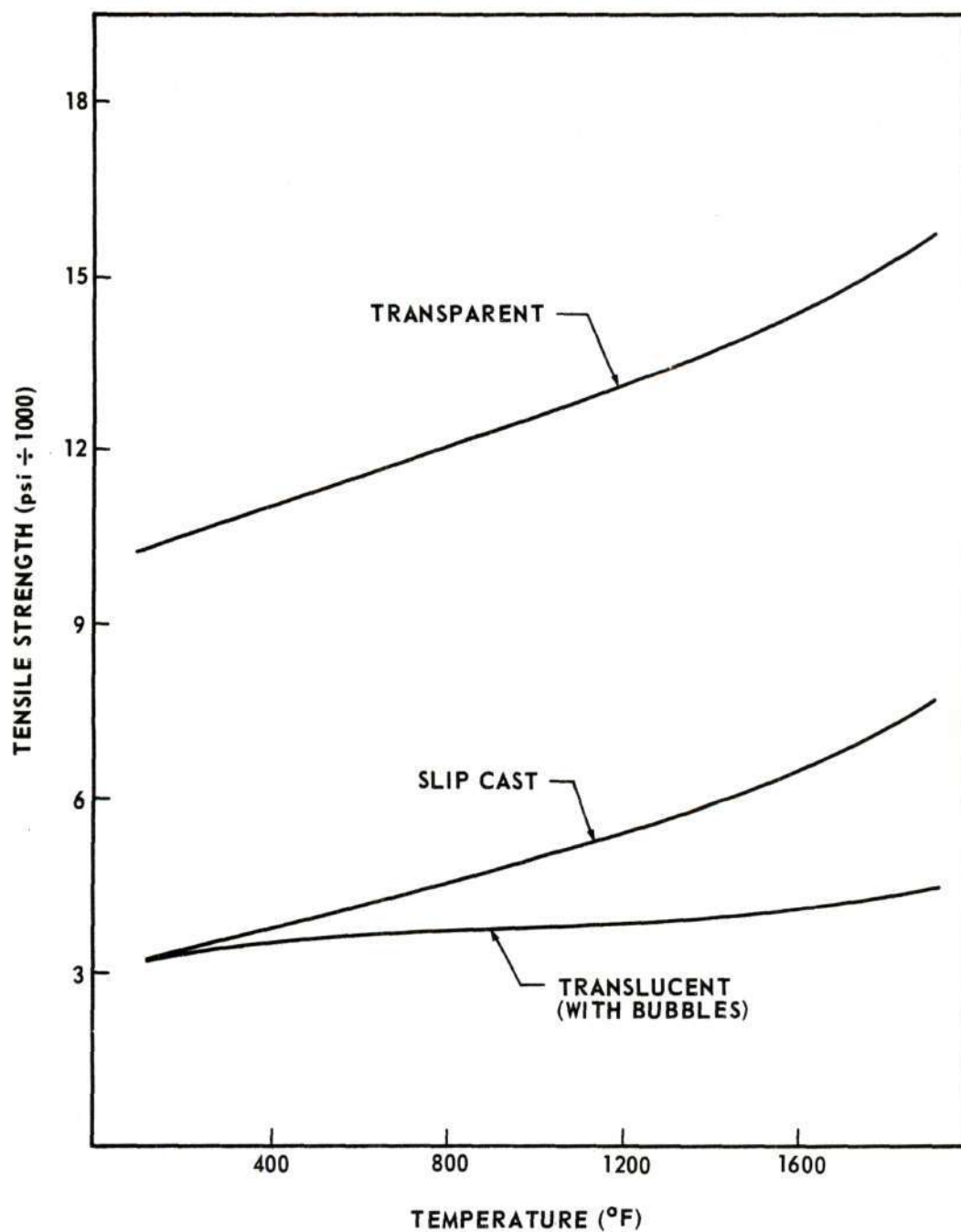


Figure 5. Elevated Temperature Tensile Strengths of Various Forms of Silica

## CHAPTER III

### INSTRUMENTATION AND EQUIPMENT

Norelco X-Ray Diffraction Facility - Used to determine cristobalite contents and to measure crystallite strain in composite specimens.

Numico Air Porosimeter - Used for measurements of bulk density, porosity, and theoretical density.

Baldwin and Instron Universal Test Machines - Used in conjunction with 4-point flexure test facility to determine modulus of rupture.

Resonant Frequency Measurement Facility - Used to measure elastic modulus.

This facility included:

1. Audio frequency generator, range 10 to 100,000 hertz.
2. 30-watt stereo-amplifier.
3. 30-watt PA, driver.
4. Phonographic pick-up arm with high output magnetic cartridge.
5. Frequency counter, with digital readout and counting gates of 1 and 10 seconds.

## CHAPTER IV

### PROCEDURE

#### Introduction

The most successful experiments conducted by the investigators previously mentioned relied on the development of compressive stresses in the surface of the ceramic composition to effect strength increases. Therefore, the approach of strengthening slip-cast fused silica with similar techniques seemed desirable. The inherent low thermal expansion characteristics of this material suggested practical limitations to the development of lower expansion glazes. A technique which would give the same end results would be to cause the center of the body to shrink (at some stage in processing) more than the exterior. Potential methods to accomplish this are (a) to quench the surface faster than the interior to produce stresses similar to those in quenched glasses, (b) to produce a composite with a greater sintering shrinkage on the interior than on the surface, or (c) crystallization of a secondary phase on the interior.

The first concept would require the ability to relieve stress during cooling in the center of the composite until the surface had reached a state of rigidity. It is unlikely that any significant surface stresses may be developed using this technique on fused silica because of its extremely low thermal

expansion. Also, the relative rigidity of this material at sintering temperatures (2100-2300°F) would tend to prevent relief of stresses developed in the core as the surface contracts during cooling.

However, using multiple casting techniques, as described in Experimental Techniques (page 23), and different particle size slips, a possibility existed that the second technique might accomplish the desired goal, providing the differential sintering characteristics of these slips were not eliminated through annealing during the sintering operation.

The crystallization phenomena described by Sosman provided an alternate approach to the formation of stresses using differential shrinkage techniques. It appeared possible to fabricate a composite specimen with a core having a higher cristobalite content than the skin. Cooling a silica composite having a fused silica skin and a cristobalite core through the inversion temperature would provide the shrinkage differences required to form a prestress condition. The magnitude of these stresses, particularly in the pure cristobalite phase, would be sufficient to destroy the composite completely. However, a composite which had fused silica as the main phase for both components, but having some cristobalite on the interior core should provide the net expansion difference required to stress the surface without causing internal failure of the composite.

#### Approach

Two concepts for the development of compressive prestress in the



surface of slip-cast fused silica were investigated experimentally. These pre-stress states were to be induced by the  $\alpha$  to  $\beta$  cristobalite inversion or by the differential sintering shrinkage of castings prepared from silica particle suspensions having different particle sizes. The selection of slips for this study, therefore, was based on particle size considerations and devitrification rate information. This information was available for several commercially produced fused silica slips in the slip characterization records at the High Temperature Materials Laboratory of the Engineering Experiment Station, Georgia Institute of Technology. A summary of this information on the three slips selected for this study is presented in Table 1. The physical characteristics of slip number 1 are typical of most commercially available slips. Slip numbers 2 and 3 are high purity slips which have a significantly lower devitrification rate than number 1. Slip number 3 also had a smaller particle size than either numbers 1 or 2. The slips were supplied by Thermo Materials Corporation, Atlanta, Georgia. Preliminary experiments were conducted on each of these slips to verify and supplement these characterization data.

Approximately 200 specimens were cast from each of the three slips for preliminary sintering characterization studies. Single component specimens were cast, dried, and sintered at several temperatures to determine relationships between processing variables and physical characteristics such as drying and firing shrinkage, elastic modulus, modulus of rupture, density, porosity, and cristobalite content. These properties are listed in Table 2.

Table 1. Characterization Data on Selected Fused Silica Slips,  
and Test Specimens Produced Using Them

Characteristic	Slip No. 1	Slip No. 2	Slip No. 3
<u>Slip Properties</u>			
Sediments (mm) in one liter after 5 hours (in 1000-ml graduate cylinder)	2.5	2.1	1.2
Weight Per Cent Solids	82.0	82.7	82.3
<u>Apparent Viscosity* (centi-poise)</u>			
60 rpm	76	155	223
30 rpm	75	162	287
12 rpm	120	220	390
6 rpm	130	280	400
pH	6.0	4.6	4.6
Mean Particle Size ( $\mu$ )	6.5	5.5	3.5
<u>Spectrographic Analysis (ppm)</u>			
Mg	Trace?	--	2-20
Fe	10-30	5-10	5-10
Ti	10-20	--	--
Al	--	Trace?	Trace?
Residual Cristobalite (per cent)	0	0.08	0.22
<u>Fired Properties</u>			
Elastic Mod. ( $\text{psi} \times 10^{-6}$ )	$5.06 \pm 0.04$	$7.71 \pm 0.04$	
Compressive Strength (psi)	$31,200 \pm 3600$	$32,409 \pm 5730$	
Modulus of Rupture (psi)	$4010 \pm 1330$	$4899 \pm 9.24$	
Porosity (per cent)	$12.49 \pm 1.30$	$7.48 \pm 0.29$	
Bulk Density (gm/cc)	$1.966 \pm 0.032$	$2.039 \pm 0.009$	
Theoretical Density (gm/cc)	$2.247 \pm 0.006$	$2.204 \pm 0.009$	
Sintering Time (hours)	4	20	
Per Cent Cristobalite	13.3	2.67	
* Measured with Brookfield Syncro-lectric Model LVF with No. 2 spindle.			



Table 2. Slip Characterization Data Obtained from  
2300°F Sintering Temperature

	Time at Temperature (minutes)		
	0	90	300
<u>Slip No. 1</u>			
Porosity (per cent)	14.36 ± 0.96	12.43 ± 0.5	12.01 ± 0.95
Bulk Density (gm/cc)	1.925 ± 0.025	1.991 ± 0.011	2.026 ± 0.016
Theoretical Density (gm/cc)	2.248 ± 0.014	2.274 ± 0.017	2.305 ± 0.007
Elastic Mod. (psi × 10 <sup>-6</sup> )	4.600 ± 0.062	5.057 ± 0.087	3.222 ± 0.036
Modulus of Rupture (psi)	4663 ± 711	4243 ± 531	3903 ± 317
Cristobalite Content (per cent)	5.0	20.01	50.18
Linear Firing Shrinkage (per cent)	---	2.02	2.54
<u>Slip No. 2</u>			
Porosity (per cent)	15.04 ± 0.34	13.22 ± 0.58	7.92 ± 0.83
Bulk Density (gm/cc)	1.931 ± 0.044	19.83 ± 0.015	2.082 ± 0.024
Theoretical Density (gm/cc)	2.273 ± 0.052	2.285 ± 0.011	2.261 ± 0.008
Elastic Mod. (psi × 10 <sup>-6</sup> )	4.598 ± 0.199	6.599 ± 0.040	8.126 ± 0.083
Modulus of Rupture (psi)	5011 ± 549	4342 ± 485	3278 ± 485
Cristobalite Content (per cent)	<0.5	2.47	5.26
Linear Firing Shrinkage (per cent)		2.56	3.55
<u>Slip No. 3</u>			
Porosity (per cent)	14.09 ± 0.39	11.01 ± 0.74	3.12 ± 1.19
Bulk Density (gm/cc)	1.950 ± 0.014	2.006 ± 0.005	2.141 ± 0.025
Theoretical Density (gm/cc)	2.270 ± 0.015	2.254 ± 0.022	2.210 ± 0.042
Elastic Mod. (psi × 10 <sup>-6</sup> )	5.204 ± 0.212	7.521 ± 0.112	8.670 ± 0.928
Modulus of Rupture (psi)	5652 ± 995	3650 ± 707	3278 ± 485
Cristobalite Content (per cent)	<0.5	2.63	4.75
Linear Firing Shrinkage (per cent)	---	2.82	4.58

Note: All data presented as a range depict the 95 percent confidence interval determined statistically for the number of specimens tested. The number of specimens used for these calculations varied from 5 to 20. Single values reported are averages calculated from 2 to 3 data points.

These data were applied to the casting of composite cylindrical test specimens having the desired relationships between the skin and the core of the specimen.

The preliminary sintering experiments were conducted in a large rotating hearth furnace. This furnace was used for the initial characterization studies since it had the best temperature uniformity.

For the bulk of the studies it was intended to use a bottom-loading furnace. The bottom-loading feature was essential to the program to provide more flexibility for cooling or quenching specimens. However, because of furnace breakdowns and associated delays, four different bottom-loading furnaces were used in the experimental phase. The different operating characteristics of these furnaces made it difficult to duplicate completely the cycles from one furnace to another. In addition to programmed variations in sintering temperature, sintering time and cooling procedure, these unavoidable furnace variations introduced additional uncertainties into the analysis of results.

The initial slip characterization studies also included composite specimens prepared with different skin thicknesses. The final sintering experiment conducted in the rotating hearth furnace had  $\frac{3}{4}$ -inch diameter composite bars with skins ( $\frac{1}{16}$ -,  $\frac{1}{8}$ -,  $\frac{3}{16}$ -, and  $\frac{1}{4}$ -inch thick) cast from slip number 2 and cores from either slip number 1 or slip number 3.

By use of slip numbers 2 and 3, composite castings with the desired differential firing shrinkage characteristics were prepared. These composites were produced by starting the casting operation with slip number 2 having the

larger particle diameter to form the skin and replacing this slip with the smaller particle size slip (number 3) having greater sintering shrinkage. The thickness of the exterior skin of the composite was controlled using casting rate information and casting durations determined from single component experimental castings.

Identical techniques were used to fabricate composites from slip numbers 1 and 2. The surface layer was cast with slip number 2 and the core from slip number 1. The casting cycles for each type of composite were varied for initial evaluations. This was done in order to establish a relationship between strength and relative cross sections between the core and the skin of the composite. Specimens for each type composite were prepared with four different skin thicknesses ( $\frac{1}{16}$ ,  $\frac{1}{8}$ ,  $\frac{3}{16}$ , and  $\frac{1}{4}$  inch).

These composites were sintered simultaneously under conditions established by the preliminary sintering studies conducted on the single-component test specimens. Additional single-component specimens were used to provide a standard for comparisons.

The results of these experiments were used to determine the optimum geometric configuration for each composite type. These results, presented in Table 3, indicate that the least scatter and highest strengths occurred with a skin thickness of approximately  $\frac{1}{8}$  inch. Additional composites were then prepared using casting cycles designed to provide optimum thickness ratios between the skin and the core of the composite. The effect of variations in the



Table 3. Modulus of Rupture Results from Studies on Thickness of Skin for Composites (Three Specimens Each)\*

Skin Thickness (in. )	Composite Slip 2 Over 1	Composite Slip 2 Over 3
$\frac{1}{16}$	4312 4870 4478 Average 4554	See Note 1
$\frac{1}{8}$	5611 5774 5643 Average 5676	6313 5347 6183 Average 5948
$\frac{3}{16}$	5767 ** **	6057 5034 5925 Average 5672
$\frac{1}{4}$	See Note 2	5919 2271** 2328**

\*All specimens were fired to 2300°F in rotating hearth furnace, with 0 hold time, and slow cooled in furnaces.

\*\* Failure propagated from internal casting flaws.

Note 1. Casting flaws and excessive drying shrinkage prevented fabrication of these specimens, as bars broke on removal from mold.

Note 2. Irregularities in skin thickness of these castings resulted when skin casting times were extended for this set, causing localized failures in casting during drying and firing cycles.

sintering parameters and subsequent cooling cycles was then investigated. Standard specimens from each basic slip were treated simultaneously with each group of composites. Fifteen different sintering cycles were used, including quenching and interrupted cooling cycles. These sintering variations are described in Table 4 with batch identification number and composite type.

Mechanical property data (Experimental Techniques, page 28), on these specimens are presented in Tables 5 through 9. Specimens were sliced along the longitudinal axis to a depth of 1 inch, and changes in diameter across the end of the specimen, perpendicular to the slot, were related to stress state (Experimental Techniques, page 31, for details of test). These data are presented in Table 10. X-ray diffraction peak-shifting experiments were also used in an attempt to substantiate these stress measurements. The results from these experiments were inconclusive because of the presence of varying quantities of cristobalite in a stress-free state as well as in a stressed state.

### Experimental Techniques

#### Specimen Preparation

Preparation of Plaster Molds. Polished stainless steel bars 7 inches long and  $\frac{3}{4}$  inch in diameter were used inside 2-inch diameter vinyl tubing as forms for the plaster molds. An aluminum plug was inserted in the bottom of vinyl tube, and the bars were positioned in the center of the tube by inserting the bars in a hole located in the center of the aluminum plug. The vinyl tube was split down the side to facilitate removal of the finished plaster mold.

Table 4. Sintering Schedules, Batch Numbers, and Compositions

Series Number	Sintering Schedule	Batch No.	No. of Specimens	Composition
1000	Fired in large rotating hearth furnace at High Temperature Materials Laboratory (HTML), Chamblee, Georgia. 2300°F, not held, slow cooled in furnace.	1001	8	Slip 1
		1002	8	Slip 2
		1003	8	Slip 3
		1010	8	Slip 2 over 1
		1011	3	Slip 2 over 1
		1020	9	Slip 2 over 3
1100	Fired in large rotating hearth furnace at HTML. Held 90 minutes at 2300°F, slow cooled in furnace.	1101	20	Slip 1
		1102	20	Slip 2
		1103	20	Slip 3
1200	Fired in large rotating hearth furnace at HTML. Held 300 minutes at 2300°F, slow cooled in furnace.	1201	20	Slip 1
		1202	20	Slip 2
		1203	15	Slip 3
2000	Fired in bottom-loading furnace, Redstone Arsenal, Alabama (RSA). Held 120 minutes at 2200°F, slow cooled in furnace. (Note: Specimens were loaded when the furnace was at 1800°F.)	2001	8	Slip 1
		2010	11	Slip 2 over 1
		2002	8	Slip 2
2100	Fired in bottom-loading furnace, RSA. Held 180 minutes at 2200°F, slow cooled in furnace. (Note: Specimens were loaded when the furnace was at 1800°F.)	2101	8	Slip 1
		2110	11	Slip 2 over 1
		2102	8	Slip 2



Table 4 (continued)

Series Number	Sintering Schedule	Batch No.	No. of Specimens	Composition
2200	Fired in bottom-loading furnace, RSA. Held 360 minutes at 2200°F, slow cooled in furnace. (Note: Specimens were loaded when the furnace was at 1800°F.)	2201	9	Slip 1
		2210	13	Slip 2 over 1
		2202	9	Slip 2
2300	Fired in bottom-loading furnace, RSA. Held 480 minutes at 2200°F, slow cooled in furnace. (Note: Specimens were loaded when the furnace was at 1800°F.)	2301	10	Slip 1
		2310	10	Slip 2 over 1
		2302	10	Slip 2
3000	Fired in bottom-loading furnace, HTML. Held 20 minutes at 2300°F, slow cooled in furnace. (Note: Specimens were loaded when the furnace was at 1800°F.)	3001	11	Slip 1
		3010	9	Slip 2 over 1
		3002	3	Slip 2
3100	Fired in bottom-loading furnace, HTML. Held 45 minutes at 2300°F, slow cooled in furnace. (Note: Specimens were loaded when the furnace was at 1800°F.)	3101	13	Slip 1
		3110	15	Slip 2 over 1
		3102	13	Slip 2
		3120	4	Slip 2 over 3
		3121	3	Slip 2 over 3
		3103	11	Slip 3
3200	Fired in bottom-loading furnace, HTML. Held 120 minutes at 2300°F, slow cooled in furnace. (Note: Specimens were loaded when the furnace was at 1800°F.)	3201	6	Slip 1
		3210	5	Slip 2 over 1
		3202	7	Slip 3

Table 4 (continued)

Series Number	Sintering Schedule	Batch No.	No. of Specimens	Composition
00X	Fired at 2300°F, air and water quenched from small bottom-loading furnace at the School of Ceramic Engineering.	001	4	Slip 1
		002	4	Slip 2
		003	4	Slip 3
		010	7	Slip 2 over 1
		020	4	Slip 2 over 3
100	Fired at 2150°F for 6 hours in small bottom-loading furnace, HTML, water quenched.	101	3	Slip 1
		102	3	Slip 2
		103	3	Slip 3
		110	7	Slip 2 over 1
		120	4	Slip 2 over 3
200	Fired at 2300°F in small bottom-loading furnace in the School of Ceramic Engineering, held at 45 minutes, furnace cooled to 300°F and held at 300°C for 20 additional hours and furnace cooled.	201	3	Slip 1
		202	3	Slip 2
		203	3	Slip 3
		210	5	Slip 2 over 1
		220	5	Slip 2 over 3
300	Fired at 2300°F, held 45 minutes in small bottom-loading furnace at the School of Ceramic Engineering, quenched in water.	301	3	Slip 1
		302	3	Slip 2
		303	3	Slip 3
		310	5	Slip 2 over 1
		320	5	Slip 2 over 3

Table 4 (continued)

Series Number	Sintering Schedule	Batch No.	No. of Specimens	Composition
500	Fired as 300, with still air quench.	501	4	Slip 1
		502	4	Slip 2
		510	13	Slip 2 over 1

Table 5. Modulus of Rupture Data Depicting Decreased  
Standard Deviation Exhibited by Composites

Batch No. and Specimen Identification	No. of Specimens	Mod. of Rupture (95 per cent CI - psi)	Std. Dev.
1001, Slip No. 1	8	4663 $\pm$ 711	850
1010, Slip No. 2 over Slip No. 1	3	5676 $\pm$ 214	86
1002, Slip No. 2	8	5011 $\pm$ 549	658
3102, Slip No. 2	13	4794 $\pm$ 382	633
3121, Slip No. 2 over Slip No. 3	3	6832 $\pm$ 105	42
3103, Slip No. 3	11	5432 $\pm$ 872	1479

Table 6. Physical Properties for Specimens  
Fired in Furnace with Rotating Hearth

Time (minutes)	Temperature (° F)	Batch	N	MOR (psi)	Std. Dev.	Density (gm/cc)
0	2300	1001	8	4663	850	1.905
0	2300	1010	3	5676	86	
0	2300	1011	3	4554	286	
0	2300	1002	8	5011	658	1.878
0	2300	1020	7	5856		
0	2300	1003	8	5652	1190	1.950
90	2300	1101	20	4243	1135	1.984
90	2300	1102	20	4342	1035	1.957
90	2300	1103	20	3650	1509	2.006
300	2300	1201	20	3903	678	2.024
300	2300	1202	19	3278	1005	2.043
300	2300	1203	13	1839	597	2.141

Table 7. Data on Specimens Sintered at 2200° F  
(in Bottom-Loading Furnace)

Time (minutes)	Temperature (° F)	Batch	N	MOR (psi)	Std. Dev.	Density (gm/cc)
120	2200	2001	8	4152	558	1.892
120	2200	2010	11	3891	735	1.892
120	2200	2002	8	4131	668	1.885
180	2200	2101	7	5293	936	1.948
180	2200	2110	11	4554	1874	1.956
180	2200	2102	8	4814	927	1.934
360	2200	2201	9	5705	851	1.968
360	2200	2210	13	5119	1027	1.961
360	2200	2202	8	4330	450	1.950
480	2200	2301	8	4012	1174	1.964
480	2200	2310	10	4711	1273	1.951
480	2200	2302	10	5436	1434	1.938

Table 8. Physical Properties for Specimens Fired at  
2300° F (in Bottom-Loading Furnace)

Time (minutes)	Temperature (° F)	Batch	N	MOR (psi)	Std. Dev.
20	2300	3001	11	4019	568
20	2300	3010	9	5176	913
20	2300	3002	2	6274	494
45	2300	3101	13	3790	
45	2300	3110	15	5210	540
45	2300	3102	13	4794	633
45	2300	3120	4	3813	737
45	2300	3121	3	6882	42
45	2300	3103	11	5432	1299
120	2300	3201	6	4949	1837
120	2300	3210	5	3899	1302
120	2300	3202	7	3655	1776



Table 9. Modulus of Rupture Data for Quenched Specimens

Batch No.	No. of Specimens	Mod. of Rupture (95 per cent CI - psi)
101	4	2950 $\pm$ 792
110	7	3009 $\pm$ 557
102	4	3530 $\pm$ 1972
120	6	3130
001-W	1*	1335
010-A	2*	5006
010-W	6	3432 $\pm$ 534
020-A	2*	2228
020-W	*	
003-A	*	
201	2	3315
210	6	2340 $\pm$ 271
202	3	2549
220	3	2750
203	1*	3890
301	*	
310	4	1981 $\pm$ 639
302	1*	5570
320	2	3800
303	*	
501	3	4621 $\pm$ 455
510	13	4958 $\pm$ 553
502	4	3690 $\pm$ 1121

\* Additional specimens fractured during quenching.

Table 10. Deflections Measured in Slotted Bar Stress Relief Test

Batch No.	Composition	Diameter Change (in. )	Remarks
1010	Slip 2 over 1	-0.0004	$\frac{1}{16}$ -inch skin
1010	Slip 2 over 1	-0.0002	$\frac{1}{16}$ -inch skin
1010	Slip 2 over 1	-0.0003	$\frac{1}{16}$ -inch skin
1010	Slip 2 over 1	-0.0006	$\frac{1}{8}$ -inch skin
1010	Slip 2 over 1	-0.0005	$\frac{1}{8}$ -inch skin
1010	Slip 2 over 1	-0.0006	$\frac{1}{8}$ -inch skin
1010	Slip 2 over 1	-0.0003	$\frac{3}{16}$ -inch skin
1010	Slip 2 over 1	-0.0004	$\frac{3}{16}$ -inch skin
1020	Slip 2 over 3	-0.0003	$\frac{1}{8}$ -inch skin
1020	Slip 2 over 3	+0.0001	$\frac{1}{8}$ -inch skin
1020	Slip 2 over 3	-0.0006	$\frac{1}{8}$ -inch skin
1020	Slip 2 over 3	-0.0010	$\frac{3}{16}$ -inch skin
1020	Slip 2 over 3	-0.0010	$\frac{3}{16}$ -inch skin
1020	Slip 2 over 3	-0.0009	$\frac{3}{16}$ -inch skin
1020	Slip 2 over 3	-0.0001	$\frac{3}{16}$ -inch skin
1020	Slip 2 over 3	-0.0005	$\frac{1}{4}$ -inch skin
1020	Slip 2 over 3	-0.0005	$\frac{1}{4}$ -inch skin
3101	Slip 1	+0.0002	Values typical for all castings from Slip 1
3101	Slip 1	-0.0001	
3101	Slip 1	-0.0001	
3102	Slip 2	0.0000	Slight inward de- flections indicate some compressive stresses for single component high purity slips
3102	Slip 2	-0.0003	
3102	Slip 2	-0.0003	
3103	Slip 3	-0.0004	
3103	Slip 3	-0.0005	
3103	Slip 3	-0.0003	

Table 10 (continued)

Batch No.	Composition	Diameter Change (in. )	Remarks
3110	Slip 2 over 1	-0.0008	
3110	Slip 2 over 1	-0.0009	
3110	Slip 2 over 1	-0.0008	
3121	Slip 2 over 3	-0.0010	This group of specimens had largest deflections due to relief of compressive stresses and also had highest MOR values with least standard deviation
3121	Slip 2 over 3	-0.0009	
3121	Slip 2 over 3	-0.0006	

Note: Diameter decreases, illustrated by negative sign, indicate relief of a compressional prestress in surface when specimen is slotted in longitudinal direction.

Using Bestwall K-59 pottery plaster (55.3 per cent) and a tap water (44.7 per cent) mixture, 10 molds were prepared at a time. The finished molds were then air-dried at 80-90° F for a minimum of 7 days.

Slip-Casting of Specimens. A silicone grease was applied to the bottom of each plaster mold. Each mold was then placed on a small glass plate. The grease was used to prevent escape of the slip from the bottom of the mold during the casting operation. A reservoir for the slip was formed on top of the mold by wrapping scotch tape around the outside and above the mold. After the casting operation was completed, the cap formed as the reservoir solidified

was immediately removed to minimize mechanical restraints of the casting as it dried in the mold (approximately 12 hours). The bars were then pushed from the molds and allowed to air dry.

Drying of Slip-Cast Bars. The cast specimens were allowed to air dry for a minimum of 24 hours, followed by 4 to 6 hours in a dryer at 125 to 150° F. To complete the drying operation, the bars were placed in another dryer at 325° F for a minimum of 2 hours. Specimens to be evaluated in the as-cast condition were then removed to a desiccator to cool prior to evaluation. Other specimens were taken directly to the furnace for firing.

Sintering Procedures. Sintering parameters investigated included temperature, heating and cooling rates, and times at temperatures. Specific temperatures ranged from 2100 to 2300° F with time at temperature varied from 0 to 480 minutes. Cooling conditions investigated included furnace cooling, water and air quenches, and combinations, as described in Table 4.

#### Evaluation of Specimens

Mechanical Property Measurement. Complete dimensional analysis was conducted on representative bar specimens from each slip at each stage in processing. This was accomplished in order to determine the characteristic shrinkage associated with each casting, drying, and firing operation. Porosity, bulk density, and theoretical density measurements were also made on as-cast and fired bars using the air displacement technique with Numico equipment. Analyses of these data for the three slips were used to determine optimum



firing conditions for each slip. The elastic modulus for each fired specimen was determined by use of sonic techniques described by Spinner and Tefft (25). Modulus of Rupture (26) measurements were made by using a four-point loading fixture and a universal testing machine. The loading fixture utilized  $\frac{1}{8}$ -inch diameter dowel pins at the contact points. The inside loading points were swivel mounted to produce uniform load distribution between the points.

Analysis of physical property data included calculation of mean values, standard deviations, 95 per cent confidence intervals. Data for composites were compared with single components by use of Variance (F) tests (27).

X-ray Diffraction Measurements. Single peak (200), integrated counting X-ray diffraction techniques were used to measure the relative cristobalite content for the fired specimens. Table 11 gives cristobalite reflections extracted from A.S.T.M. Powder Diffraction File. Quantitative data were generated by comparing individual specimen scans with identical measurements made on a 100 per cent cristobalite standard, supplied by the High Temperature Materials Laboratory. The cristobalite standard had been prepared by sintering a block of fused silica at 2700° F for 86 hours, which was sufficient to convert all the silica to cristobalite. Since the specific reflection (200) used for these analyses corresponds closely to the amorphous hump of fused silica, a correction factor was required to produce exact quantitative measurements. As this correction was relatively small, it was not utilized for the values reported in Table 2 for slip characterization.

Attempts were also made to demonstrate the presence of stresses in the



Table 11. ASTM Powder Index Data for Cristobalite

Relative Intensity	d (Å)	(Lkl)
100	4.050	101
20	2.485	200
13	2.841	102
11	3.135	111
7	1.870	212

fired bars using X-ray diffraction techniques. The cross sections of several specimens were positioned in the goniostat and diffraction angles, for the cristobalite (200) peak were determined. This angle was compared with the angle observed for powder (unstrained) specimens. Using Bragg's Law,  $n\lambda = 2d \sin \theta$ , increased angles of diffraction (or higher  $\sin \theta$  values) would require decreased d-spacings for the particular planes of diffraction and thereby indicate the presence of a compressive stress in the crystal phase. The relationships between stress, strain, modulus of elasticity, and Poisson's ratio are described by Cullity (28) and Azaroff (29), and for measurements of stress in the center of these composite cylinders reduce to:

$$(a) \text{ Strain} = \epsilon = \frac{\Delta d}{d_0}$$

$$(b) \text{ Stress} = \sigma = \frac{\epsilon E}{2\gamma}$$

with E = modulus of elasticity,  $\gamma$  = Poisson's ratio.

Slotted-Rod Stress Analysis. The slotted-rod test described by Kirchner was used on several specimens. A thin (0.032 inch) diamond saw blade cut was made through the longitudinal axis of the bar, as depicted in Figure 6.

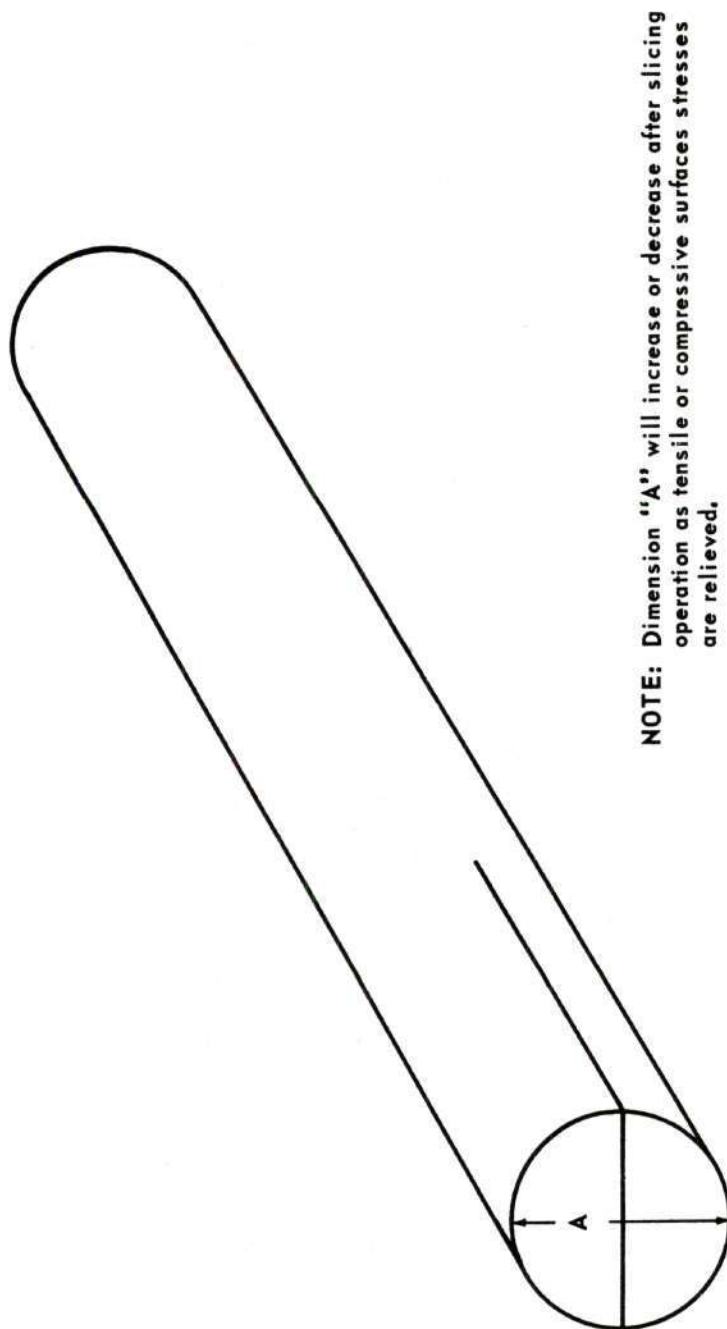


Figure 6. Illustration of Split Rod Test

Measurements of the diameter of the bar were made before and after slicing.

Increased diameters indicated presence of tensional prestress in the surface, while decreased diameters indicated relief of compressional surface prestress.

Results of these tests are presented in Table 10.

## CHAPTER V

## DISCUSSION OF RESULTS

The amount of prestress which could be obtained in a composite having a  $\frac{1}{8}$ -inch skin thickness with a core diameter of  $\frac{1}{2}$  inch was calculated. The calculation was based on variations in cristobalite content between the skin and the core. The core was assumed to contain 15 per cent cristobalite and the change in specific volume of the cristobalite during the  $\alpha$  and  $\beta$  inversion was the mechanism causing stress. The cristobalite content for the skin was assumed to be 1.5 per cent. These cristobalite contents correspond to the comparative devitrification rates observed for slip numbers 1 and 2 as presented in characterization data presented in Table 2.

- Assuming: (1)  $E_{\text{core}} \text{ (elastic modulus core)} = E_{\text{skin}} \text{ (elastic modulus skin)}$ ,  
 (2) Uniform temperature distribution throughout specimen.  
 (3) Only longitudinal stresses.

The stressed induced in the surface:

$$\sigma_{\text{skin}} = - \left( K_{\text{core}} - K_{\text{skin}} \right) \frac{E}{1-\gamma} \frac{A_{\text{core}}}{A_{\text{total}}}$$

with:  $K = \text{(per cent cristobalite) (linear contraction during } \alpha \text{ to } \beta \text{ inversion)}$

$$K_{\text{skin}} = 0.024 \text{ percent}$$

$$K_{\text{core}} = 0.24 \text{ percent}$$

$$\nu = \text{Poisson's ratio} = 0.155$$

$A_c$  = area core and  $A_T$  = total cross sectional area.

Therefore:

$$\sigma_s = -\left(K_c - K_s\right) \frac{E}{1-\nu} \cdot \frac{A_c}{A_T} = -0.22 \frac{6 \times 10^6}{0.845} \frac{4}{9} = -6.9 \times 10^3 \text{ psi},$$

where the (-) sign describes compressive stress state.

These calculations represent a maximum prestressing capability and do not reflect the effects of localized crystallite or crystallite-glass interface fracture during phase inversion. The various sintering conditions evaluated were attempts to eliminate or decrease the probability of fracture in cristobalite regions and to maintain physical integrity between the fused silica and cristobalite phases.

Evidence that some stresses were generated in the composite specimens prepared with the higher cristobalite content in the center was found in both the X-ray diffraction measurements and the slotted rod test. Two separate peaks were observed in the immediate vicinity of  $22.0^\circ$  ( $2\theta$ ). However, these measurements were not reproducible from specimen to specimen, and no definite trends were observed. Inward deflections were also noted in the slotted rod test which indicated the relief of compressive surface stresses by the longitudinal slot in the end of the specimen. Deflections of 0.0001 to 0.0010



inch were observed. Slight inward deflections of 0.0001 to 0.0002 inch were experienced with the specimens prepared with number 1 slip and deflections from 0 to 0.0005 inch were observed for the high purity slips 2 and 3. Maximum inward deflections were obtained for the 2 over 3 composite specimens (batch number 3121) of 0.0009 to 0.0010 inch. These data (Table 10) for the composite specimens with  $\frac{1}{8}$ -inch skin (minimum) all exhibit larger contraction in diameters than the single-phase specimens, qualitatively demonstrating the presence of a potentially useful prestress.

Additional evidence demonstrating the development of stresses during sintering and subsequent cooling is shown in Figures 7 and 8. The cup and cone fractures illustrated in Figure 7 occurred when specimens were over-fired and/or cooled too rapidly through the inversion temperature. These failures were attributed to the development of tensile cracks on the interior of the specimen as the specific volume of the core decreased during cooling. These cracks then propagated to the surface on 45-degree shear diagonals. Figure 8 illustrates the effect of casting a reverse composite with the higher processing shrinkage occurring on the surface. For this specimen the number 1 slip was used for the skin and the number 2 slip the core. As shown in the photograph, the surface layer crazed as the bar cooled and contracted more rapidly than the core. These photographs illustrate the differences in sintering shrinkage characteristics exhibited by the high purity and conventional fused silica slips.

Tables 3 through 9 list physical properties and specimen information for

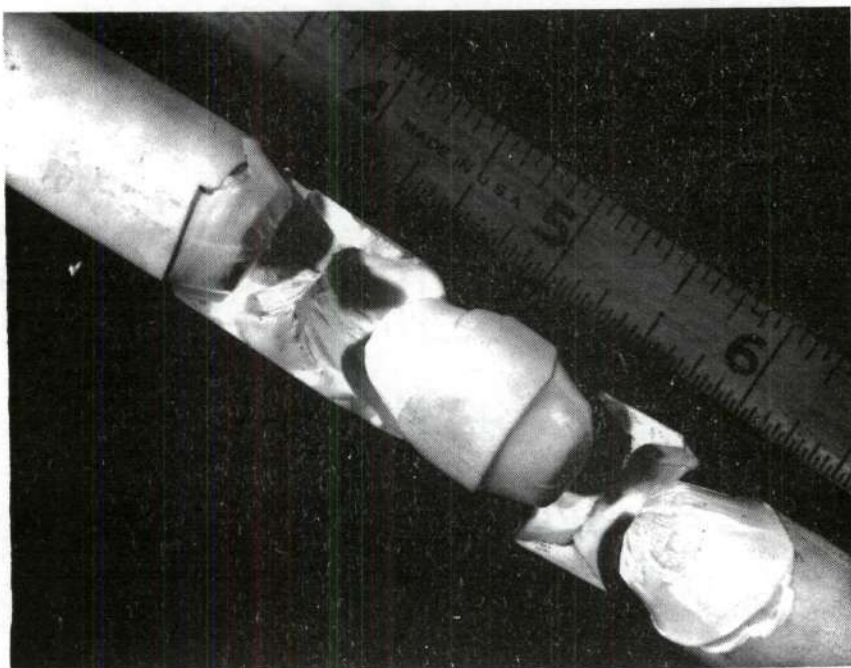


Figure 7. Composite Specimen, Slip 2 Over 1

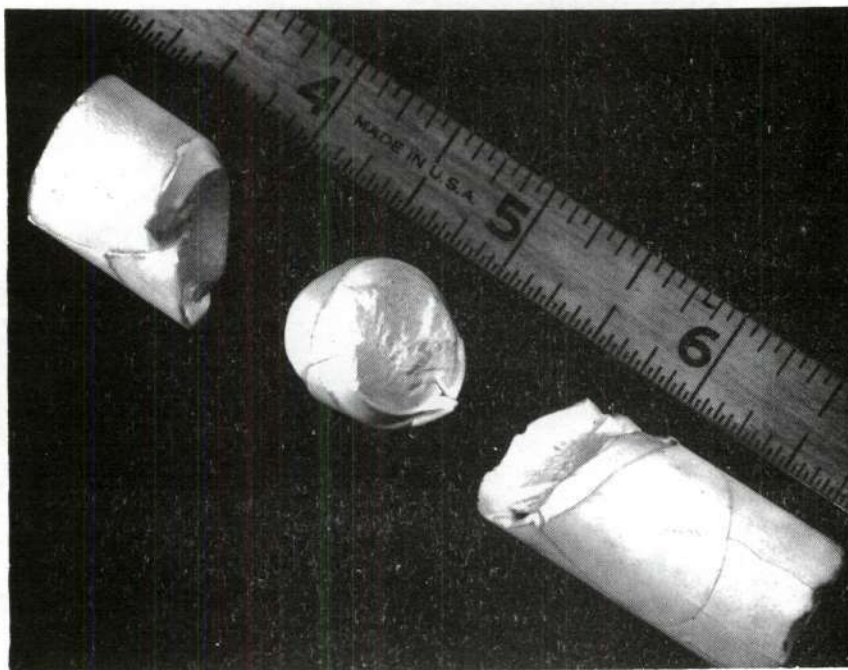


Figure 8. Composite Specimen, Slip 1 Over 2

the composite and single-phase specimens. Two batches of composite specimens (numbers 1010 and 3121) showed significant improvement in physical properties when compared with single-phase specimens. The average modulus of rupture values for these composites shows slight numerical increases. However, the calculated standard deviation from the average is an order of magnitude better for the composites, as illustrated in Table 5. The slightly higher averages are relatively insignificant, considering the scatter associated with measurements for the standard single component specimens. The order of magnitude decrease in standard deviation exhibited by the composite has great significance, especially to the designer. Design values are based on the mean versus a multiple of the standard deviation. The multiple factor is determined by the performance reliability desired.

These high strength specimens were slow-cooled inside the furnaces. Although different furnaces were used, the sintering temperature was 2300° F for both sets of specimens. The 2 over 1 composites were held at temperature for 0 time while the 2 over 3 composites were held at temperature for 45 minutes. The total sintering effects were approximately the same for both batches because of different heating and cooling characteristics of the two furnaces.

Statistical analysis (F-test) of the variance data for these composites indicated the variance obtained for the single component specimens was greater than the variance calculated for the composite (at a level of significance of 98



and 99 per cent, respectively).

Table 9 lists the modulus of rupture data obtained for specimens cooled under conditions other than in the furnace. All specimens subjected to quench in water from any temperature above 1000° F either were fractured during quenching or developed flaws which led to significant strength reductions (from 50 to 75 percent). The air-quenched specimens (500 series) were not as significantly affected. The composites from slip number 2 over slip number 1 were relatively unaffected by air quench, whereas single component specimens showed significant reductions in strength when air-quenched. No significant difference was apparent between these composites, when air-quenched and furnace-cooled. Interrupted cooling with a hold just above (300°C) the inversion temperature resulted in a significant strength decrease in all composite or single component specimens.

Data for sintering temperature variations were not conclusive, but maximum strengths for each type of specimen (composites and single phase) were obtained at 2300° F temperature. The optimum sintering duration appeared to be a function of the characteristics of the furnace used, as well as the specific slips used. Figure 9 graphically presents average modulus of rupture values for slip numbers 1 and 2 as a function of time and temperature.

The smaller particle size distribution for slip number 3 led to a casting problem which caused it to be dropped from the study shortly after the slip characterization phase was completed. The drying shrinkage observed for slip



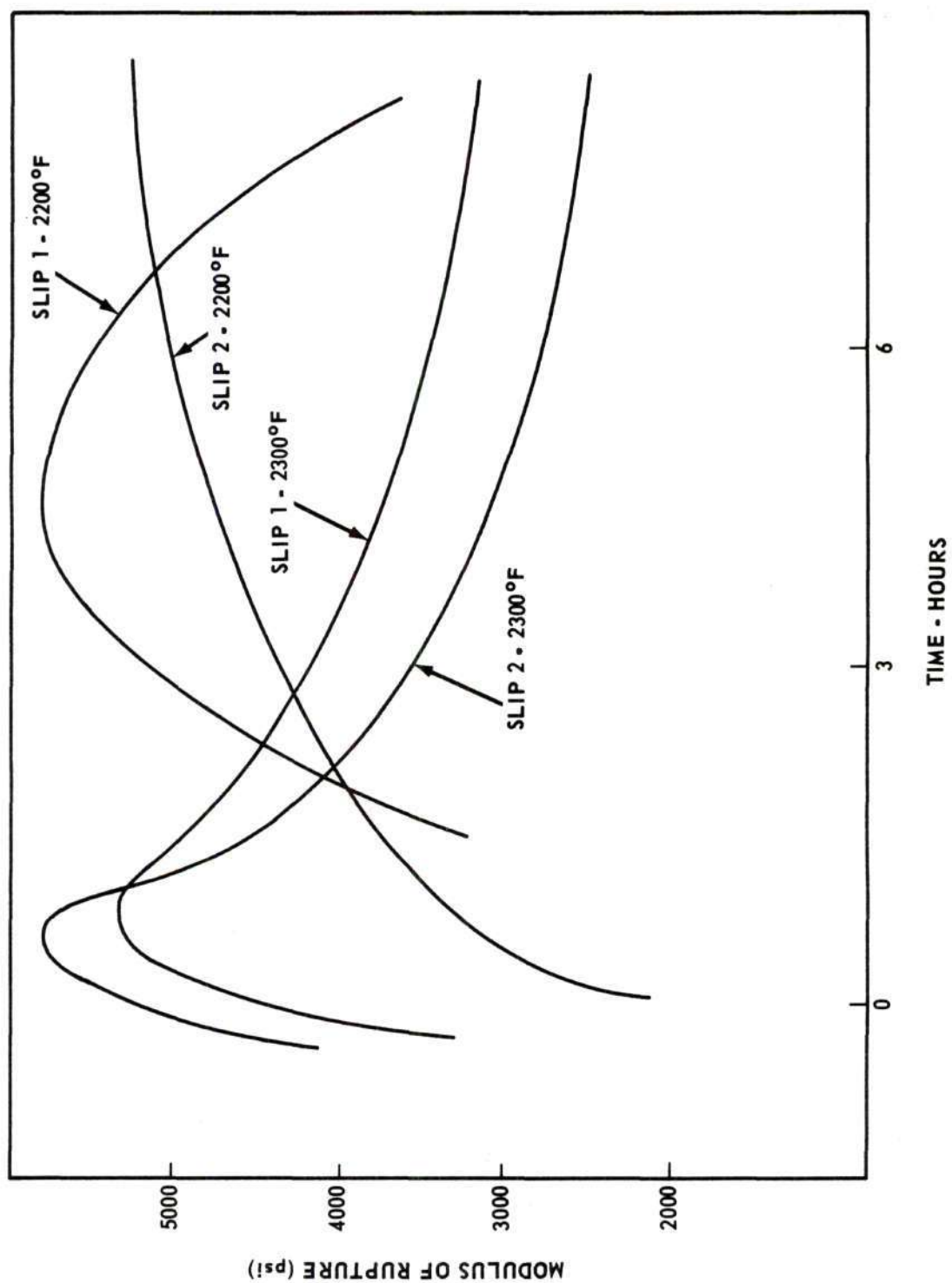


Figure 9. Modulus of Rupture Versus Time at Sintering Temperature

number 3 was approximately 0.7 per cent compared to 0.19 and 0.08 for numbers 2 and 1 respectively. This caused failures during the drying cycles for composites produced with this slip. These failures sometimes occurred as complete fracture of the bar and sometimes only as invisible microcracks which later opened up during sintering operations. The difference in drying shrinkage between slip number 1 and 3 was apparently marginal in respect to overstressing the composite in the drying stage, since several composites of this type were successfully produced. In fact, batch number 3121, 2 over 3, exhibited the highest average strength and the least scatter of any group of specimens. It would therefore appear that the two-particle size approach to prestressing is feasible. However, future experimenters should select slips with slightly less different particle sizes to reduce the desirable drying shrinkage differences.

## CHAPTER VI

### CONCLUSIONS

1. The experimental results of this study indicate the feasibility of reducing the scatter in the strengths observed for slip-cast fused silica. Two separate batches showed order of magnitude decreases in the calculated standard deviations for mean strength of composite type specimens when compared with single phase specimens identically processed. The composites batches 1010 and 3121 had standard deviations of 86 and 42 respectively, compared with 860 and 633 for single phase specimens.

2. Composites produced with higher cristobalite content in the core than in the skin had a slightly higher mean modulus of rupture than either of the individual components: 5676 psi compared to 4633 psi and 5011 psi. The calculated standard deviation for the mean modulus of rupture was 86, compared with 850 and 658, respectively.

3. Composites produced with the smaller particle size slip (number 3) in the core and the larger particle size (number 2) for the skin also had a higher mean for the modulus of rupture: 6832 psi compared with 4794 psi and 5432 psi for slip numbers 2 and 3, respectively. Again the standard deviation for the composite, 42, was significantly lower than either single phase materials 633 and 1299 for slip numbers 2 and 3, respectively.

4. In addition to the modulus of rupture values, the presence of a stressed condition was demonstrated by the inward deflections observed with the slotted bar test. The presence of double reflections at about 22.0 degrees for some composite specimens studied in the X-ray peak shifting experiments also indicated a stressed condition. The normal cristobalite peak occurs at 21.95 degrees, and reflections were measured at angles slightly offset (from 0.1 to 0.2 degree) as well as this angle. This indicates that some of the cristobalite in the center of the specimen was in tension.

5. Analysis of the photographs (Figures 7 and 8) of specimens which cracked during the cooling cycle reveals the cause of the cracking to be differences in contraction rates for the core and skin of the composites. Qualitatively, the type of cracking experienced is directly relatable to the predicted stress state. The excessive magnitude of the contraction differences or the rate the specimen cooled caused these failures. However, the photographs alone confirm the feasibility of developing stresses in a composite as originally postulated.



## BIBLIOGRAPHY

## Literature Cited

- (1) Pears, Coultas D., and Digesu, Frank J., "The True Stress-Strain Properties of Brittle Materials to Very High Temperatures," Southern Research Institute, Birmingham, Ala. (September 13, 1963).
- (2) "Ceramic Processing," Publication 1576, National Academy of Sciences, Washington, D. C., LCCC 68-600017 (1968).
- (3) Hall, Richard C., "Strengthening Ceramic Materials," American Ceramic Society Bulletin, 47, 251-258 (March 1968).
- (4) Fletcher, Peter C., and Tillman, J. J., "Effect of Silicone Quenching and Acid Polishing on the Strength of Glass," Journal of the American Ceramic Society, 147, 379-382 (August 1964).
- (5) Weymann, H. O., "A Thermoviscoelastic Description of the Tempering of Glass," Journal of the American Ceramic Society, 45, 517-522 (November 1962).
- (6) Barsom, J. M., "Fracture of Tempered Glass," Journal of the American Ceramic Society, 51, 75-78 (February 1968).
- (7) Duke, D. A., Megeles, J. E., Jr., Macdowell, J. F., and Bobb, H. F., "Strengthening Glass Ceramics by Application of Compressive Glazes," Journal of the American Ceramic Society, 51, 98-102, 111 (February 1968).
- (8) Kirchner, H. P., Gruver, R. M., Platts, D. R., Risbel, P. S., and Walker, R. E., "Chemical Strengthening of Ceramic Materials," Summary Report, Linden Laboratories, Inc., State College, Pa. (April 1968).
- (9) Kirchner, H. P., et al., "Chemical Strengthening of Ceramic Materials," Second Quarterly Report, Linden Laboratories, Inc., State College, Pa. (November 1964).

- (10) Kirchner, H. P., et al., "Chemical Strengthening of Ceramic Materials," Summary Report, Linden Laboratories, Inc., State College, Pa. (April 1967).
- (11) Kistler, S. S., "Stresses in Glass Produced by Nonuniform Exchange of Monovalent Ions," Journal of the American Ceramic Society, 45, 59-68 (February 1962).
- (12) Nordberg, M. E., Mochel, E. L., Garfunkel, H. M., and Olcott, J. S., "Strengthening by Ion Exchange," Journal of the American Ceramic Society, 97, 215-219 (May 1964).
- (13) Sosman, Robert B., "The Properties of Silica," American Chemical Society Monograph Series, Chem. Cat. Co., Little and Ives, N.Y., 1927.
- (14) Wilson, Hewitt, "Ceramics-Clay Technology," 1st Edition, McGraw-Hill, N. Y., 1927.
- (15) Corning Glass Works, Corning, N. Y., in Lab 1 Product Brochure, Industrial Publication, 1967.
- (16) Sosman, R. B., "The Phases of Silica," Rutgers University Press, New Brunswick, N. J., 1965.
- (17) Day, Sosman, and Hostetter, American Journal of Science, 4, 1-39 (1914).
- (18) Wagstaff, Frank Everton, "Kinetics of Crystallization of Vitreous Silica," Doctoral Thesis, University of Utah, August 1962.
- (19) Murphy, C. A., "Characterization of Fused Silica Slips," Special Technical Report No. 2, Engineering Experiment Station, Georgia Institute of Technology, April 1968.
- (20) Fleming, J. D., Boland, Paul, and Harris, J. N., "Porosity Measurements by Air Displacement," Materials Research and Standards (January 1963).
- (21) Brown, S. D., and Kistler, S. S., "Devitrification of High Silica Glasses of the System  $\text{Al}_2\text{O}_3\text{-SiO}_2$ ," Journal of the American Ceramic Society, 42, 263-270 (June 1959).

- (22) Boland, Paul, and Fleming, J. D., "The Effect of Firing Atmosphere on the Sintering of Slip Cast Fused Silica," presented at 65th Annual Meeting of American Ceramic Society, May 1963.
- (23) Uhlman, D. R., "Glasses and Glass-Ceramic Materials," to be published in book "Elasticity, Plasticity, and Structure of Matter," second edition, Cambridge University Press, 1969 (?).
- (24) Fleming, J. D., "Fused Silica Manual," Final Report Project No. B-153, Engineering Experiment Station, Georgia Institute of Technology, September 1964.
- (25) Spinner, S., and Tefft, W. E., "A Method for Determining Mechanical Resonance Frequencies and for Calculating Elastic Moduli from These Frequencies," ASTM Proc 61, 1221-1238 (1961).
- (26) ASTM Handbook, Part 5, pp. 688-690, 1961.
- (27) Natrella, M. G., NBS Handbook No. 91, "Experimental Statistics," Chapter 2, U. S. Dept. of Commerce, August 1963.
- (28) Cullity, B. D., "Elements of X-ray Diffraction," pp. 431-451, Addison-Wesley Publishing Co., Inc., Reading, Mass., 1967.
- (29) Azaroff, L. V., "Elements of X-ray Crystallography," pp. 558-568, McGraw-Hill, Inc., N. Y., N. Y., 1968.

#### Other References

- (1) Berry, T. F., Allen, W. C., and Hassett, W. A., "Role of Powder Density in Dry Pressed Ceramic Parts," Ceramic Bulletin, 38 (1959).
- (2) Lennon, Brockway, Bowers, et al., "A Survey of Firing Processes and Their Critical Influence on Ceramics," AFML-TR-65-281, October 1965.
- (3) Fleming, J. D., Johnson, J. W., Boland, Paul, Bomar, S. H., and Colcond, A. R., "Materials for High Temperature Nuclear Engineering Applications," Summary Report No. 1, Project No. B-153, June 1962.
- (4) Hochman, R. F., and Fleming, J. D., "Orientation of Cristobalite Formed on Surfaces of Amorphous Silica Plates," Journal of the American Ceramic Society, 47 (February 1964).



- (5) Miller, D. G., Singleton, R. H., and Wallace, A. V., "Metal Fiber Reinforced Ceramic Composites," Ceramic Bulletin, 45 (1966).
- (6) Poulos, N. E., Murphy, C. A., Corbett, W. J., et al., "Development of Lightweight Broadband Radomes from Slip-Cast Fused Silica," AFAL-TR-67-56, April 1962.
- (7) Sucor, Eugene W., "Diffusion of Oxygen in Vitreous Silica," Journal of the American Ceramic Society, 46, 14-19 (January 1963).
- (8) Thummler, F., and Thomma, W., "The Sintering Process," Metallurgical Reviews, Review 115, The Metals and Metallurgy Trust, 1967.